Journal of Radioanalytical and Nuclear Chemistry (2020) 324:903–911
https://doi.org/10.1007/s10967-020-07089-6

Investigation of Se(IV) diffusion in compacted Tamusu clay by capillary method

Hao Wu[1] · Wei Huang[1] · Zhiqin Duan[1] · Mingbiao Luo[1,2] · Zhifen Wang[3] · Rong Hua[3]

Received: 21 January 2020 / Published online: 7 March 2020

Abstract
For the first time in laboratory, diffusion parameters of Se(IV) in the clay of Chinese Tamusu region(TMS clay) against compacted density, ionic strength and pH value were obtained by capillary method. Diffusion process can be Simplified by using one-dimensional semi-infinite medium diffusion model. The results show a good similarity with the international literature and meet the internationally recognized range of 10^{-9}–10^{-12}. This work will provide data support and theoretical references for the pre-selection of clay rock sites in China's high-level radioactive waste deep geological repository.

Keywords Se(IV) · Tamusu clay · Diffusion · High level waste disposal

Introduction

Deep geological disposal is currently the most safe and reliable high-level radioactive waste disposal method recognized by the international community. Due to the high self-sealing property, low porosity and low permeability, claystone is also as a candidate surrounding rock for disposal of high level radioactive waste, which is valued by many scholars [1–3]. In addition to the Beishan granite pre-selection site in Gansu Province, China started the pre-selection of clay rock underground repository site in 2009. Up to now, a lot of achievements have been made in the research on the engineering characteristics and hydrogeology of claystone [4, 5]. Tamusu area is the primary pre-selected site of clay rock disposal reservoir. It is located in Alashan, Inner Mongolia, China, with dry climate and little rain, and high degree of rock consolidation. Cl–SO_4–Na type or Cl–SO_4–Na–Ca type water is the mainly type of groundwater. The pH value of groundwater is between 7.75 and 9.86, the average value is 8.3, and the Eh value is between − 23.2 and − 162.3 mv [6]. These studies provide certain data and theoretical support for the construction of the repository. However, the engineering characteristics and hydrological research are not enough. It is also necessary to evaluate the diffusion behavior of key nuclides in geological media.

^{79}Se is one of the key nuclides for the safety assessment of the repository [7]. Se is mainly present in the form of SeO_3^{2-} and $HSeO_3^-$ in aqueous solution, and its adsorption on the clay surface is small, and migration easily occurs [8]. Many outstanding scholars have done a lot of great work on the migration and adsorption behavior of Se. Jan et al. [9] studied the migration behavior of Se(IV) in crushed granite under the condition of mixed groundwater and mixed seawater(length: 2 cm) and obtained the apparent/effective diffusion coefficient (D_a/D_e) in groundwater. The apparent/effective diffusion coefficients (D_a/D_e) in groundwater were 1.73×10^{-10} m^2 s^{-1} and 1.02×10^{-10} m^2 s^{-1}, respectively, and in seawater were 1.02×10^{-10} m^2 s^{-1} and 3.06×10^{-11} m^2 s^{-1}, respectively. Jussi et al. [10] obtained the effective diffusion coefficient of Se oxyanions in granitic rock, and the results showed that the De of Se was significantly higher for Grimsel graodiorite (GG); De = $(2.5\pm1.5)\times10^{-12}$ m^2 s^{-1} than for Kuru grey granite (KGG); De = $(7\pm2)\times10^{-13}$ m^2 s^{-1} due to the higher permeability of GG compared with KGG. Li et al. [11] developed the research of sorption of Se species

✉ Mingbiao Luo
luomingbiao_ecut@126.com

✉ Rong Hua
rhua@ecit.cn

[1] College of Chemical Biology and Materials Science, East China University of Technology, Nanchang 330013, Jiangxi, China

[2] State Key Laboratory of Nuclear Resources and Environment, East China University of Technology, Nanchang 330013, Jiangxi, China

[3] College of Nuclear Science and Engineering, East China University of Technology, Nanchang 330013, Jiangxi, China

on mineral surfing. Experimental results show that the distribution coefficients (K_d values) of Se(IV) on the rock and mineral samples increased with the decreasing of Se(IV) concentration. Videnská et al. [12] made research on the adsorption behavior of SeO_4^{2-} and SeO_3^{2-} on the fragmentary granite, and it showed that no pollution was recorded in the case of SeO_4^{2-}. However, the significant sorption was found for SeO_3^{2-},and the coefficient of the distribution is 0.2–2.5 and 0.2–12.7 $cm^3\ g^{-1}$. He et al. [13] had made research on the influence of Fe(II) on the Se(IV) sorption under oxic/anoxic conditions using bentonite. They found that Fe(II) species could greatly enhance the sorption efficiency of Se(IV) via bentonite,meanwhile, Under anoxic conditions, Se(IV) can be reduced by a two-step sorption/reduction mechanism. He et al. [14] Studied sorption of Se on TMS clay in simulated groundwater with high salinity under aerobic/anaerobic conditions. They pointed out that K_d values in aerobic conditions were higher than those in anaerobic conditions, and the change trend of the K_d values was not affected by oxygen. Moreover, Se sorption was promoted at alkaline conditions. Of course, there are many outstanding achievements that are not listed one by one. However, none of these studies deals with the diffusion behavior of Se in TMS claystone.

The radionuclide diffusion process under actual geological conditions is shown in Fig. 1. In the complex geological environment, the repository may be destroyed. Groundwater enters the repository by the means of the fractures and brings dissolved nuclides into the biosphere. At present, the most widely used method to simulate the nuclide diffusion experiment in laboratory is diffusion method [15–17]. This method can well get the experimental data of nuclide from the beginning of diffusion to the steady state of diffusion, and can better demonstrate the dynamic process of nuclide diffusion [18, 19]. However, this method's device is usually complex and the experimental period is relatively long, which leads to the increase of the uncontrollable factors in the experimental process and increases the difficulty of the experiment [20–22]. In this paper, the diffusion behavior of Se(IV) in TMS clay has been studied by capillary method. The experimental equipment is relatively simple, and the experimental period is short. The results obtained are in good agreement with those in the literature [23, 24]. Through a series of the experiments, the key parameters such as diffusion coefficient and distribution coefficient are obtained, which provide a solid theoretical basis for the site selection of the deep geological repository of the claystone.

Theory

Diffusion of the nuclide in homogeneous porous media can be regarded as one-dimensional unsteady diffusion experiment, which can be described by Fick's second law:

$$\frac{\partial C}{\partial t} = D_a \frac{\partial^2 C}{\partial x^2} \tag{1}$$

where D_a is the apparent diffusion coefficient of nuclide in clay, $m^2\ s^{-1}$; C is the nuclide concentration at x from the solution-clay contact interface, mol L^{-1}; C_0 is the nuclide concentration at the solution-clay contact surface, mol L^{-1}; t is the diffusion time, s; x is the diffusion distance, m.

Under the conditions of constant partition coefficient, stable nuclide concentration at the solution-clay interface and semi-infinite boundary conditions, that is, under this experimental condition, the numerical solution of formula (1) is as follows:

$$\frac{C}{C_0} = erfc\left(\frac{x}{2\sqrt{D_a t}}\right) \tag{2}$$

The boundary condition is:

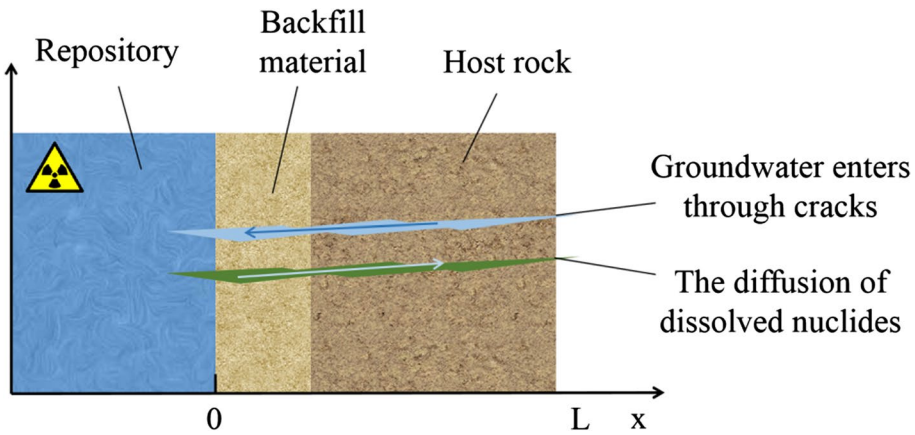

Fig. 1 Radionuclide diffusion process under actual geological conditions

$$\begin{aligned} C(0,0) &= C_0, \ldots t = 0, \quad x = 0 \\ C(x,0) &= 0, \ldots t = 0, \quad 0 \le x \le L \\ C(0,t) &= 0, \ldots t \ge 0, \quad x = 0 \end{aligned} \tag{3}$$

Where, C_0 is the concentration of nuclide at the solution-clay interface, mol L^{-1}; *erfc* is the error complementary function:

$$erfc(z) = 1 - \frac{2}{\sqrt{\pi}} \int_0^z \exp\left(-x^2\right) dx \tag{4}$$

Experiment

Materials and reagents

In this work, the clay used was obtained from a rotating hole at a depth of 543.7-543.8 m underground in tamusu region, Inner Mongolia, China and provided by the state key laboratory of nuclear resources and environment. All the clays were screened by 200 mesh sieve. The component and chemical composition of clay powder were detected by X-ray diffraction and X-ray fluorescence. The results are shown in Fig. 2 and Table 1. We used ion chromatography to analyze tamarin groundwater from the same rotating hole depth. Components of the simulated groundwater used in the experiment are shown in Table 2.

The nuclide that is used in this study is the stable isotope ^{75}Se. 3000 mg L^{-1} of Se solution is obtained by accurately weighing 1.0538 g of selenium dioxide (aladdin biochemical technoligy co.LTD, GR) and dissolving it in a certain amount of pure water, transferring it to a 250 ml volumetric flask and constant volume to the scale line. The experiment was carried out at a constant temperature of 20 °C, and all reagents used were analytically pure.

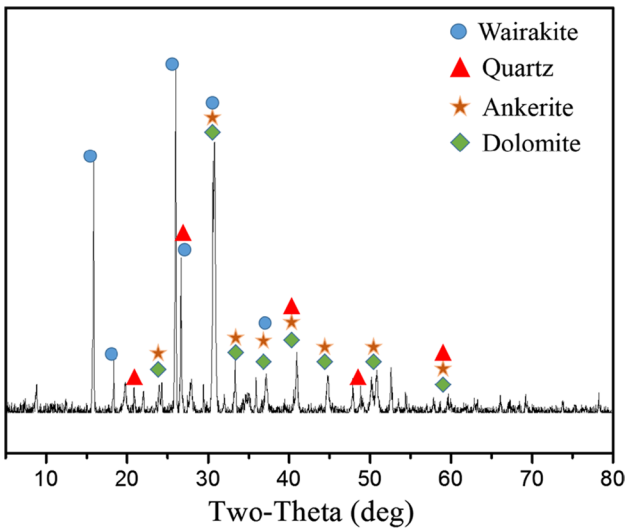

Fig. 2 XRD of TMS Clay

Table 1 Composition of TMS Clay

Composition	Wt%	Composition	Wt%
C	22.248	Si	11.063
O	44.205	S	0.6374
Na	2.1732	K	1.4725
Mg	3.8458	Ca	5.3489
Al	4.7329	Fe	4.1349

General operation procedures

TMS clay powder (200 mesh) without further purification is filled into the capillary (PEEK; length: 2 cm; inner diameter: 1 mm), and the filled capillary is put into the simulated underground water, so that it is completely submerged. Pre-experiment shows that the solution can fill the voids in the compacted clay after soaking for 5 days. After soaking in simulated underground water, It is put in a 2 ml freeze-drying tube with 1 ml Se solution and take it out after 48 h. The capillary and the clay therein were evenly cut into ten sections, and the clay was pushed out and placed in a 1 mol L^{-1} nitric acid solution, then left for 24 h and filtered. Finally ICP-OES (iCAP 7600, Thermo fisher technology co., LTD, Shanghai, China) was used for analysis. The schematic diagram is shown in Fig. 3. During the experiment, we measured the concentration of Se solution in the freeze-dried tube and found that there was almost no change. No obvious clay particles were found in the solution, and the clay powder dropped at both ends of the capillary can be ignored.

Results and discussions

XRD

The corresponding specific peaks of each component are marked in Fig. 3. It can be found that the components of TMS clay mainly include dolomite[$CaMg(CO_3)_2$], quartz[SiO_2] and clinoptilolite[$Na(AlSi_5O_{12})\cdot 4H_2O$]. Because of the existence of Fe^{2+} and Ca^{2+} ions in clay, there will be ankerite[CaMg, $Fe(CO_3)_2$].

Table 2 Component of underground water from the same hole

Component	Mass (mol L^{-1})
NaCl	0.320
Na_2SO_4	0.085
$MgCl_2$	0.019
$CaCl_2$	0.024

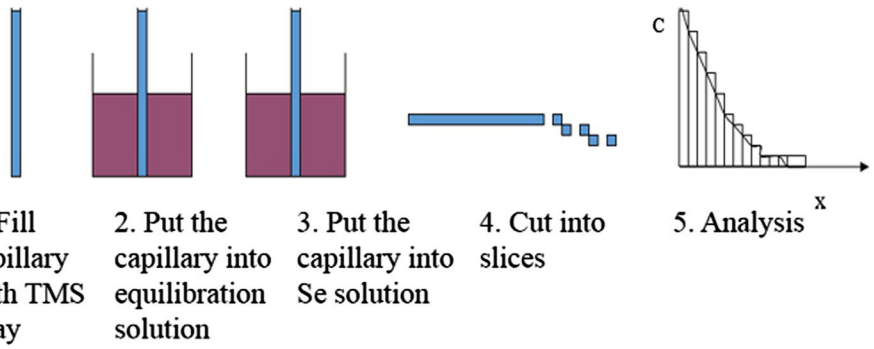

Fig. 3 Experimental diagram of capillary method

Breakthrough curve

Equation (2) was used to fit the diffusion data of Se under different compacted density, pH volues and ionic strength, and the breakthrough curves is shown in Fig. 4. The results show that the experimental data are in good agreement with the theoretical curve, which indicates that the diffusion of Se(IV) in clay can be simplified by one-dimensional semi-infinite medium diffusion theory. It also proves that it is feasible to study the diffusion behavior of selenium in TMS Clay by capillary method.

Effect of compacted densities

Porosity of the clay is closely related to its compacted density. The relationship between effective diffusion coefficient, apparent diffusion coefficient and clay porosity can be described as follows:

$$D_a = \frac{D_e}{\varepsilon + \rho_1 K_d} \tag{5}$$

where: D_a is the apparent diffusion coefficient, $m^2\ s^{-1}$; D_e is the effective diffusion coefficient, $m^2\ s^{-1}$; ε is the total porosity of compacted clay; ρ_1 is the density of compacted clay, kg m^{-3}; K_d is the distribution coefficient of nuclide.

The porosity can be obtained from $\varepsilon = 1 - \rho_1/\rho_0$ by the dry density ρ_0(~ 2600 kg m^{-3})

In capillary experiments, the total distribution coefficient can be replaced by the distribution coefficient of nuclides in the first section [25]. Therefore, K_d can be expressed as follows:

$$K_d = \frac{C_s}{C_L} = \frac{\left(C_{slice} - \varepsilon V_{slice} C_L\right)/\rho_1 V_{slice}}{C_L} \tag{6}$$

C_s is the nuclide concentration in the solid phase, mg g^{-1}; C_{slice} is the nuclide concentration in the first capillary, mg L^{-1}; C_L is the nuclide concentration in the solution, mg L^{-1}; V_{slice} is the volume of the first capillary section, m^3.

We have designed 1600 kg m^{-3}, 1750 kg m^{-3}, 1800 kg m^{-3}, 1900 kg m^{-3} and 2050 kg m^{-3} compacted

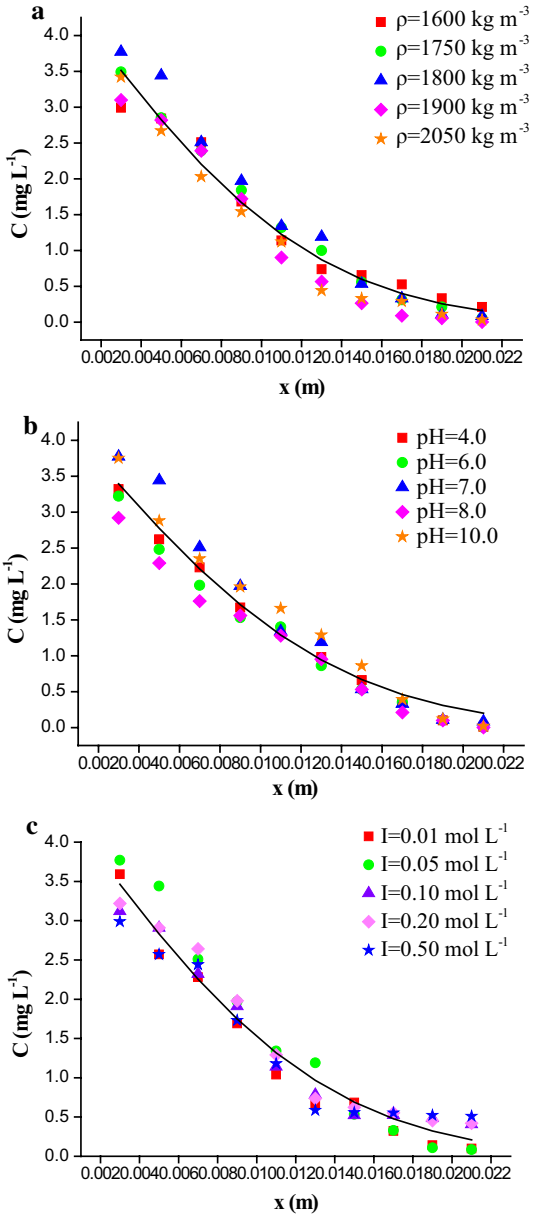

Fig. 4 Breakthrough curves of Se in TMS clay under different conditions: **a** for compacted density; **b** for pH volues; **c** for ionic strength

Table 3 Experimental conditions of clay compacted density

Project	Method/condition
Experimental method	Capillary method
Equilibration solution	Simulated groundwater
Temperature (°C)	20 ± 1
Nuclide	^{75}Se
Compacted densities (kg m^{-3})	1600, 1750, 1800, 1900, 2050
pH values	7.00 ± 0.05
Material	TMS clay

Table 4 Experimental conditions of ion strength

Project	Method/condition
Experimental method	Capillary method
Equilibration solution	Simulated groundwater
Temperature (°C)	20 ± 1
Nuclide	^{75}Se
NaCl (mol L^{-1})	0.01, 0.05, 0.10, 0.20, 0.50
pH value	7.00 ± 0.05
Compacted density (kg m^{-3})	1800 ± 20
Material	TMS clay

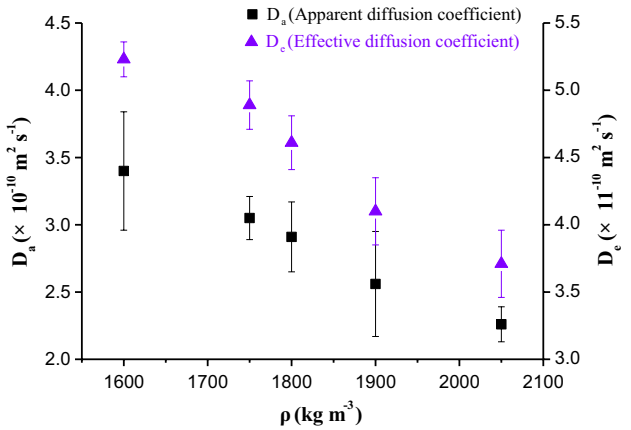

Fig. 5 Effect of compacted density on diffusion behavior

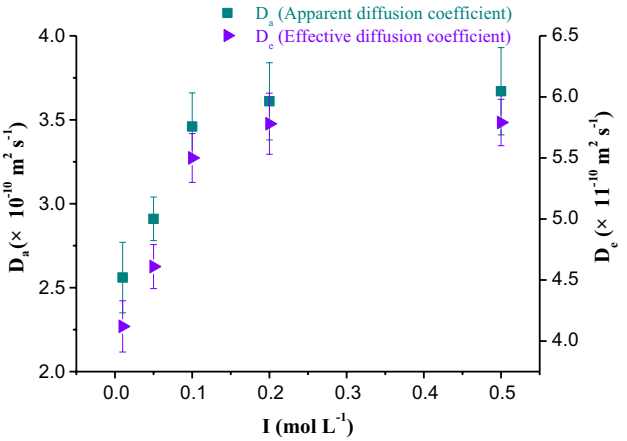

Fig. 6 Effect of ionic strength on diffusion behavior

density experiments to study the influence of different compacted density on nuclide diffusion behavior in TMS clay. See Table 3 for the specific experimental conditions. The relationship between compacted density and apparent/effective diffusion coefficient is shown in Fig. 5. As the compacted density increased from 1600 to 2050 kg m^{-3}, the apparent/effective diffusion coefficient decreased from $(3.40 \pm 0.44) \times 10^{-10}$ to $(2.26 \pm 0.13) \times 10^{-10}$ m^2 s^{-1}, $(5.23 \pm 0.26) \times 10^{-10}$ to $(3.71 \pm 0.51) \times 10^{-10}$ m^2 s^{-1} respectively. At the same time, it was found that the porosity ε of the compacted clay decreased from 0.378 to 0.205 with the increase of the compacted density. The granular layer of clay is mainly composed of a diffuse electric double layer and a free water layer [22]. It is believed that the increase of the compaction density makes the clay particle layer more compact, and the decrease of pore directly leads to the decrease of free water layer. The diffusion path of the nuclide is restricted, and the diffusion coefficient is correspondingly reduced.

Effect of ion strength

The diffusion of the Se in clay is affected not only by the pores of compacted clay, but also by the ion exclusion. NaCl solutions of 0.01, 0.05, 0.1, 0.2 and 0.5 mol L^{-1} were used to investigate the effect of ionic strength on Se(IV) diffusion behavior. The specific experimental conditions are shown in Table 4.

Ionic strength's influence on the diffusion coefficient of Se is shown in Fig. 6. With the change of ionic strength (0.01–0.5 mol L^{-1}), the apparent/effective diffusion coefficient of Se(IV) increased from $(2.56 \pm 0.21) \times 10^{-10}$ to $(3.67 \pm 0.55) \times 10^{-10}$ m^2 s^{-1}, and $(4.12 \pm 0.27) \times 10^{-11}$ to $(5.79 \pm 0.20) \times 10^{-11}$ m^2 s^{-1}. In accordance with Gouy–Chapman–Stern electric double layer theory, the thickness of the diffusion electric double layer is related to the ionic strength of the electrolyte solution. According to the Debye length calculation formula, the thickness of diffusion electric double layer can be expressed as follows:

$$k^{-1} = \frac{1}{\sqrt{8\pi\lambda_B N_A I}} = \frac{0.304}{\sqrt{I}} \quad (7)$$

where k^{-1} is the thickness of the diffusion electric double layer; N_A is the Avogadro constant; λ_B is the Bjerrum length of the medium, and λ_B is about 0.7 nm at room temperature; I is the ionic strength of the electrolyte.

Table 5 Experimental conditions of pH value

Project	Method/condition
Experimental method	Capillary method
Equilibration solution	Simulated groundwater
Temperature (°C)	20 ± 1
Nuclide	^{75}Se
pH values	4.00, 6.00, 7.00, 8.00, 10.00
Compacted density (kg m^{-3})	1800 ± 20
Material	TMS clay

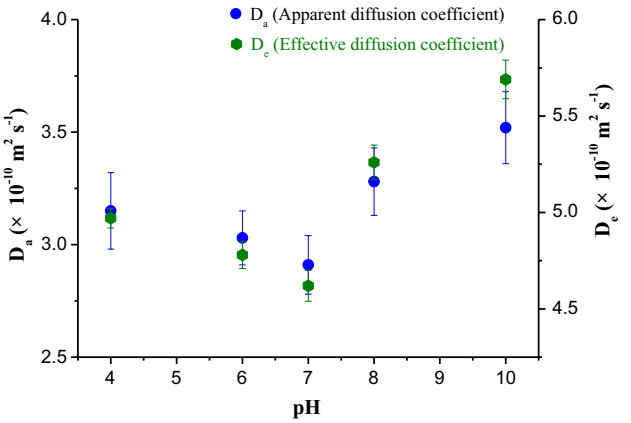

Fig. 7 Effect of pH value on diffusion behavior

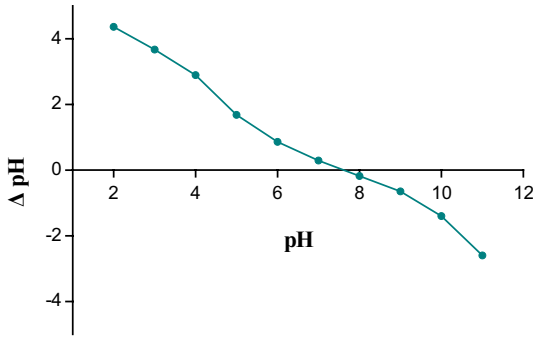

Fig. 8 Zero potential of TMS clay

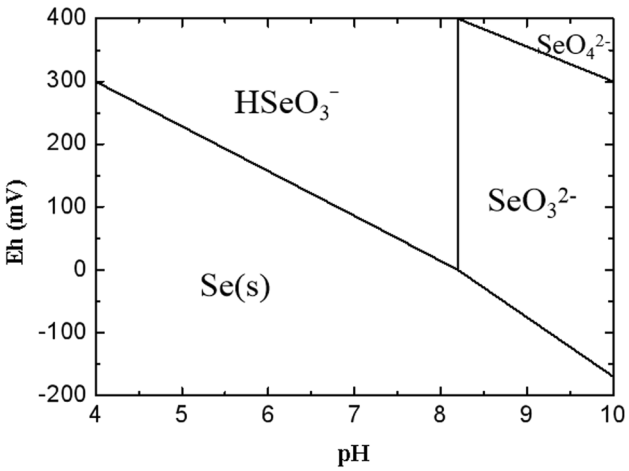

Fig. 9 Se species at different pH values [18]

Therefore, the above results can be summarized as: the increase of ionic strength results in the narrowing of diffusion double layer, the widening of pore water channel (free water layer) between clay particles, and the corresponding increase of nuclide diffusion coefficient.

Effect of pH values

The existence form of Se is mainly determined by its environment [26, 27]. We explored the effect of solution pH on the diffusion behavior of Se in clay. The specific experimental conditions are shown in Table 5.

Through the analysis of the experimental results (Fig. 7), it is found that the apparent/effective diffusion coefficients of Se decreased with the increase of pH value in the range of 4–7, which were $(3.15 \pm 0.17) \times 10^{-10}$–$(2.91 \pm 0.26) \times 10^{-10}$ m^2 s^{-1} and $(4.97 \pm 0.05) \times 10^{-10}$–$(4.62 \pm 0.08) \times 10^{-10}$ m^2 s^{-1} respectively; When the pH is in the range of 7–10, the apparent/effective diffusion coefficient of Se increased with the increase of pH value, which are $(2.91 \pm 0.26) \times 10^{-10}$–$(3.52 \pm 0.32) \times 10^{-10}$ m^2 s^{-1} and $(4.62 \pm 0.08) \times 10^{-10}$–$(5.69 \pm 0.10) \times 10^{-10}$ m^2 s^{-1} respectively. For this phenomenon, we also carried out exploratory experiments at zero potential point to explain it.

Ionic strength of the solution has made little effect on the zero potential point of the TMS clay [14]. After adding 0.04 g clay powder to 20 mL of 0.05 mol L^{-1} NaCl solution with adjusted pH value and soaking it for 48 h, it is found that the zero potential point of the clay is at pH = 7.62, as shown in Fig. 8. When the pH of the solution is less than 7.62, the clay is electropositive; when the pH of the solution is greater than 7.62, the clay is electronegative. Combining with the existing forms of Se at different pH values (Fig. 9), we can explain the above experimental results as follows: as the pH value increased from 4 to 7, Se species in solution gradually transformed into anion HSO_3^-, which interacts with the positive charge on the clay surface. At this time, adsorption predominates, diffusion behavior slows down and diffusion coefficient decreases; when the pH value is greater than 7, the forms of Se in solution are mainly SO_3^{2-} and SO_4^{2-}, which repel the negative charge on the clay surface and accelerate the diffusion. It should be mentioned here that the distribution coefficient should have decreased with

the increase electronegativity, but it actually increased. The calcium ion concentration decreased in the range of the pH values [14], so that Se was incorporated to the Ca^{2+} and CO_3^{2-} [28–30].

Comparision

At present, the pre-selected sites of high-level radioactive waste deep geological reservoir in China contain Beishan in Gansu Province, Caidamu in Xinjiang, Gaomiaozi in Inner Mongolia, and Tamusu in Inner Mongolia. Most of the domestic researches focus on granite and bentonite, and the research on claystone has just started in recent years. We compared the effective diffusion coefficient obtained in this experiment (seen in Table 6) with the results of other domestic researchers to obtain a more comprehensive and accurate evaluation [31–33], as shown in Fig. 10.

As can be seen from the figure, the effective diffusion coefficients are all distributed in the range of 10^{-9}–10^{-12}, which is consistent with the internationally recognized results. Compared with bentonite and granite, the distribution of the effective diffusion coefficient of nuclide in clay is relatively concentrated, which indicates that Se(IV) diffusion in clay is more stable and less susceptible to the impact of changes of the external environment, which is particularly important for the construction of disposal repository.

Table 6 Comparison with literature data

Project		Temperature (°C)	Porosity (ε)	$K_d \times 10^{-4}$	$D_a \times 10^{-10}$ ($m^2\ s^{-1}$)	$D_e \times 10^{-10}$ ($m^2\ s^{-1}$)
Compacted density (kg/m^3)	1600	20 ± 1	0.38	7.26	3.40 ± 0.44	5.23 ± 0.26
	1750		0.33	7.27	3.05 ± 0.16	4.89 ± 0.37
	1800		0.30	7.13	2.91 ± 0.26	4.61 ± 0.41
	1900		0.27	7.04	2.56 ± 0.39	4.10 ± 0.50
	2050		0.21	7.01	2.26 ± 0.13	3.71 ± 0.51
Ionic strength (mol/L)	0.01	20 ± 1	0.30	7.27	2.56 ± 0.21	4.12 ± 0.27
	0.05		0.30	7.13	2.91 ± 0.26	4.61 ± 0.36
	0.10		0.30	7.17	3.46 ± 0.40	5.50 ± 0.41
	0.20		0.30	7.23	3.61 ± 0.47	5.78 ± 0.50
	0.50		0.30	7.10	3.67 ± 0.55	5.79 ± 0.20
pH	4.00	20 ± 1	0.30	7.12	3.15 ± 0.17	4.97 ± 0.05
	6.00		0.30	7.10	3.03 ± 0.23	4.78 ± 0.07
	7.00		0.30	7.13	2.91 ± 0.26	4.62 ± 0.08
	8.00		0.30	7.25	3.28 ± 0.31	5.26 ± 0.09
	10.00		0.30	7.31	3.52 ± 0.32	5.69 ± 0.10

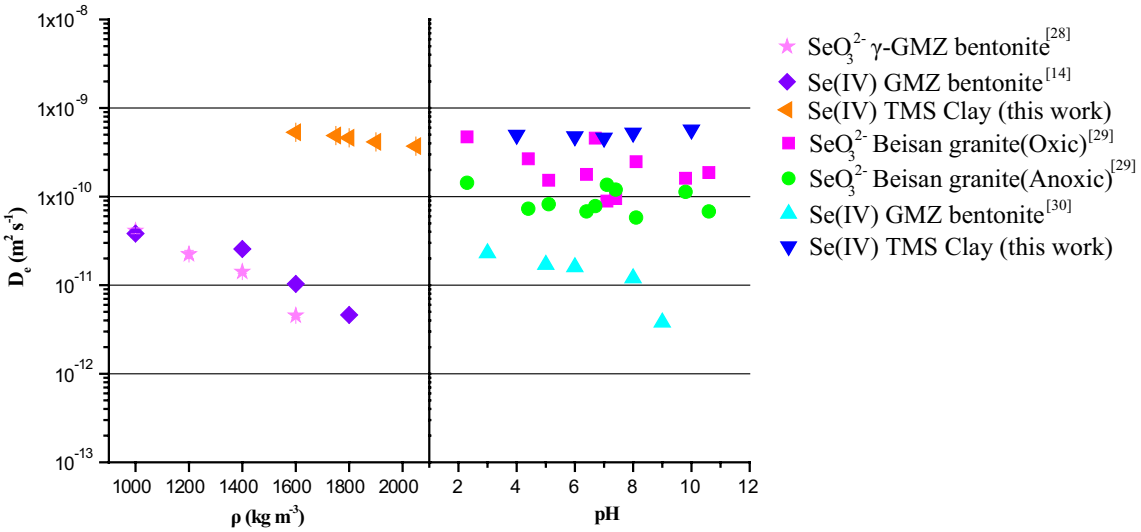

Fig. 10 Comparison with literature data

However, the effective diffusion coefficient obtained in this work is an order of magnitude larger than that obtained in other materials, which may be due to the difference in material scale between the through-diffusion method (g) and the capillary method (mg).

Conclusion

In this experiment, the research on the diffusion behavior of Se(IV) in TMS clay was carried out by capillary method. The experimental results show that the diffusion behavior of Se in TMS clay can be simplified by using one-dimensional semi-infinite medium diffusion model. With the increase of clay compaction density, apparent/effective diffusion coefficient decreases. With the increase of ionic strength, apparent/effective diffusion coefficients increase. With the increase of pH value, apparent/effective diffusion coefficient decreases first and then increases, and get to smallest at pH = 7. In the comparison of other types of disposal geological materials in China, it is found that the diffusion behavior of selenium in TMS clay was more stable, and the overall experimental results were within the range of accuracy recognized by internationally literatures. This work provides data support and theoretical support for the construction of deep geological disposal repository for high-level radioactive waste.

Acknowledgements This project was supported by the National Defense Science and Technology Foundation Project (JCKY2017401C005), Natural Science Foundation of China (201761002), Graduate Innovation Program (DHYC201912). To the best of our knowledge, the named authors have no conflict of interest, financial or otherwise.

References

1. Stéphane M, Reda Al YuC, Berthe G, Matrayb JM (2020) Study of the permeability in the Opalinus clay series (Mont Terri–Switzerland) using the steady state method in Hassler cell. J Petrol Sci Eng 184:106457
2. Mijnendonckx K, Miroslav H, Wang L, Jacops E, Provoost A, Mysara M, Wouters K, Craen MD, Leys N (2019) An active microbial community in Boom Clay pore water collected from piezometers impedes validating predictive modelling of ongoing geochemical processes. Appl Geochem 106:149–160
3. De Echave T, Tribet M, Gin S, Jégou C (2019) Influence of iron on the alteration of the SON68 nuclear glass in the Callovo–Oxfordian groundwater. Appl Geochem 100:268–278
4. Yuan GX, Zhang LQ, Zeng QL (2018) Prediction of rock mass quality in target depth for Tamusu area of Alxa pre-selected region for geological disposal of high-level nuclear waste. J Eng Geol 26:1690–1700
5. Hu HY, Liu XD, Yang T, Wang GB, Huo L (2014) Experimental study and mechanism analysis on mechanical properties of clay rocks in Tamusu area. Geotech Investig Surv 42:9–13
6. Huang HE, Xu WD, Zhang WM, Zhang QL, Wang J (2017) Groundwater chemical and isotopes characteristics of the yingejing preselected area for high level radioactive waste disposal repository. Sci Tech Engrg 17:34–40
7. Grambow B (2008) Mobile fission and activation products in nuclear waste disposal. Contam Hydrol 102:180–186
8. Koch SH, Pröhl G (2001) Considerations on the behaviour of long-lived radionuclides in the soil. Radiat Environ Biophys 40:93–104
9. Jan YL, Tsai SC, Li YY (2014) Determination of sorption and diffusion parameters of Se(IV) on crushed granite. J Radioanal Nucl Chem 301:365–371
10. Jussi I, Mikko V, Mervi S, Lalli J, Marja SK, Andrew M (2016) Sorption and diffusion of selenium oxyanions in granitic rock. Contam Hydrol 192:203–211
11. Li XD, Eini P, Jussi I, Mervi S, Antero L, Stellan H, Andrew M, Marja SK (2018) Sorption of Se species on mineral surfaces, part I: batch sorption and multi-site modelling. Appl Geochem 95:147–157
12. Videnská K, Palágyi Š, Štamberg K, Vodičková H, Havlová V (2013) Effect of grain size on the sorption and desorption of $SeO_4^{2-}$and SeO_3^{2-} in columns of crushed granite and fracture infill from granitic water under dynamic conditions. J Radioanal Nucl Chem 298:547–554
13. He JG, Shi YL, Yang XY, Zhou WQ, Li Y, Liu CL (2018) Influence of Fe(II) on the Se(IV) sorption under oxic/anoxic conditions using bentonite. Chemosphere 193:367–384
14. He HY, Liu J, Dong Y, Li HH, Zhao SW, Wang J, Jia ML, Zhang H, Liao JL, Yang JJ, Yang YY, Liu N (2019) Studied sorption of selenite on Tamusu clay in simulated groundwater with high salinity under aerobic/anaerobic conditions. J Environ Radioact 203:210–219
15. Tsai S, Ouyang S, Hsu CN (2001) Sorption and diffusion behavior of Cs and Sr on Jih-Hsing bentonite. Appl Radiat Isot 54:209–215
16. César V, Javier G, Joan DP, María M (2011) Transport of Strontium Through a Ca-bentonite(Almería, Spain) and Comparison with MX-80 Na-bentonite: experimental and Modelling. Water Air Soil Pollut 218:471–478
17. Zhao SW, Wu T, Li HH, Xu MH, Mao L, Guo YH, Liu YC, Jia ML (2019) Difusion of Re(VII) and Se (IV) in compacted GMZ bentonite in the presence of *Bacillus* spp. J Radioanal Nucl Chem 320:47–53
18. Yang XY, Ge XK, He JG, Wang CL, Qi LY, Wang XY, Liu CL (2018) Effects of Mineral Compositions on Matrix Diffusion and Sorption of ^{75}Se(IV) in Granite. Environ Sci Technol 52:1320–1329
19. Wu T, Wang ZF, Tong YH, Wang YY, VanLoon LR (2018) Investigation of Re(VII) diffusion in bentonite by through-diffusion and modeling techniques. Appl Clay Sci 166:223–229
20. NairobyA Tiziana M, Miguel GG, Ursula A, Manuel M (2011) Strontium migration in a crystalline medium: effects of the presence of bentonite colloids. J Contam Hydrol 122:76–85
21. Shih YH, Lee IH, Ni CF, Tsai TL, Chen LC, Li CP, Tsai SC, Su TY (2018) Experimental and numerical investigations of $^{99}TcO_4^-$ diffusion in compacted SPV 200 bentonite. J Radioanal Nucl Chem 316:1081–1089
22. Wigger C, Van Loon LR (2017) Importance of interlayer equivalent pores for anion diffusion in clay-rich sedimentary rocks. Environ Sci Techno 51:1992–2006
23. Wang XK, Montavon G, Grambow B (2003) A new experimental design to investigate the concentration dependent diffusion of Eu(III) in compacted bentonite. J Radioanal Nucl Chem 257:293–297
24. Montavon G, Alhajji E, Grambow B (2006) Study of the Interaction of $Ni^{2+}$and Cs^+ on MX-80 Bentonite; effect of compaction using the capillary method. Environ Sci Tech 40:4672–4679

25. Yu SM, Ren A, Wang XK (2005) Effect of pH on the apparent diffusion coefficient and sorption distribution coefficient of 152, 154 Eu(III) in compacted bentonite: a study of capillary method. J Radioanal Nucl Chem 27:104–108
26. Giffaut E, Grivé M, Blanc P, Vieillard P, Colàs E, Gailhanou H, Gaboreau S, Marty N, Made B, Duro L (2014) Andra thermodynamic database for performance assessment: thermoChimie. Appl Geochem 49:225–236
27. Scheinost AC, Charlet L (2008) Selenite reduction by mackinawite, magnetite and siderite: XAS characterization of nanosized redox products. Environ Sci Technol 42:1984–1989
28. Aurelio G, Fernandez MA, Cuello GJ, Roman RG, Alliot I, Charlet I (2010) Structural study of selenium(IV) substitutions in calcite. Chem Geol 270:249–256
29. Cowan CE, Zachara JM, Resch CT (1990) Solution ion effects on the surface exchange of selenite on calcite. Geochem Cosmochim Acta 54:2223–2234
30. Heberling F, Vinograd VL, Polly R, Gale JD, Heck S, Rothe J, Bosbach D, Geckeis H, Winkler B (2014) A thermodynamic adsorption/entrapment model for selenium(IV) coprecipitation with calcite. Geochem Cosmochim Acta 134:16–38
31. Wang ZF, Wu T, Ren P, Hua R, Wu H, Xu MH, Tong YH (2019) Through-difusion study of Se(IV) in γ-irradiated bentonite and bentonite–magnetite. J Radioanal Nucl Chem 332:801–808
32. He JG, Ma B, Kang ML, Wang CL, NieZ Liu CL (2017) Migration of ^{75}Se(IV) in crushed Beishan granite: effects of the iron content. J Hazard Mater 324:564–572
33. Wang ZF, Wang H, Li QM, Xu MH, Guo YH, Li JY, Wu T (2016) pH effect on Re(VII) and Se(IV) diffusion in compacted GMZ bentonite. Appl Geochem 73:1–7